JOURNAL OF THE BALKAN GEOPHYSICAL SOCIETY, Vol. 6, No. 4, November, 2003, p. 188 – 201.

Investigation of the Tectonic Structure of the NW Part of the Amynteon Basin (NW Greece) by means of a Vertical Electrical Sounding (VES) survey

A. Atzemoglou[(1)] , P. Tsourlos[(2)] and S. Pavlides [(2)]

[(1)] Institute of Geology and Mineral Exploration, 1 Fragon str, 54626, Thessaloniki, Greece (E-mail: matzem@thes.igme.gr)
[(2)] School of Geology, Aristotle University of Thessaloniki, 54006 Thessaloniki, Greece.

Abstract: *A large-scale VES survey was conducted at the NW part of the Amynteon basin in order to study the tectonic setting of the area. Sixty-four soundings (AB/2= 1000 m) were measured on a near-regular grid and were processed with 1-D inversion algorithm. Several parameterisation patterns were tested before producing the final interpretations. Since the measured soundings centres are situated on a regular grid it was possible to combine the 1-D interpretation results and produce pseudo-2D and 3D depth slices.*

Interpretations are in very good agreement with the existing drilling and geological information and reveal a relatively detailed picture of the basin's geological background. Further the results allowed us to verify the continuation of known faults and to obtain new structural information about the studied area. The results indicate that despite the increased use of 2D electrical surveys, 1-D VES measurements are still a very useful tool for large-scale applications.

Keywords: *Tectonic structure, VES survey, Amynteon Basin, 1-D resistivity inversion.*

INTRODUCTION

A large-scale geoelectrical sounding survey was conducted at the Amynteon Basin (N. Greece) (Fig. 1). The surveyed area is situated near the two small lakes (Zazari and Chimaditis) and between the villages of Pedino, Valtonera, Limnochori, Agrapidia and Aetos in Florina prefecture in Western Macedonia, Greece (Figure 2). The aim of this survey was to obtain structural and geological information about the basin as part of a larger survey aiming to the investigation of the low enthalpy geothermal potential of the area.

The technique of VES for prospecting 1-D structures is well established (Koefoed, 1979). A large number of fully automated 1-D interpretation algorithms for VES can be found in literature (Inman, 1975; Rijo, 1977; Zohdy, 1989, Basokur, 1990, Basokur, 1999). One of the known problems of the 1-D VES interpretations is the inherent lack of solution uniqueness (Kunetz, 1966; Koefoed, 1979). Due to this problem, practice has shown, that using fully automated inversion schemes, without taking geological conditions into account, can result into interpretations, which are mathematically correct but geologically erroneous. In this framework, approaches involving interactive semi-automated interpreting can become particularly useful in taking both the mathematical and the geological factors into consideration.

One popular way to incorporate geology into the VES automated interpretation is to provide some compact geological information (i.e. drill columns) by assuming some certain properties of geoelectrical layers

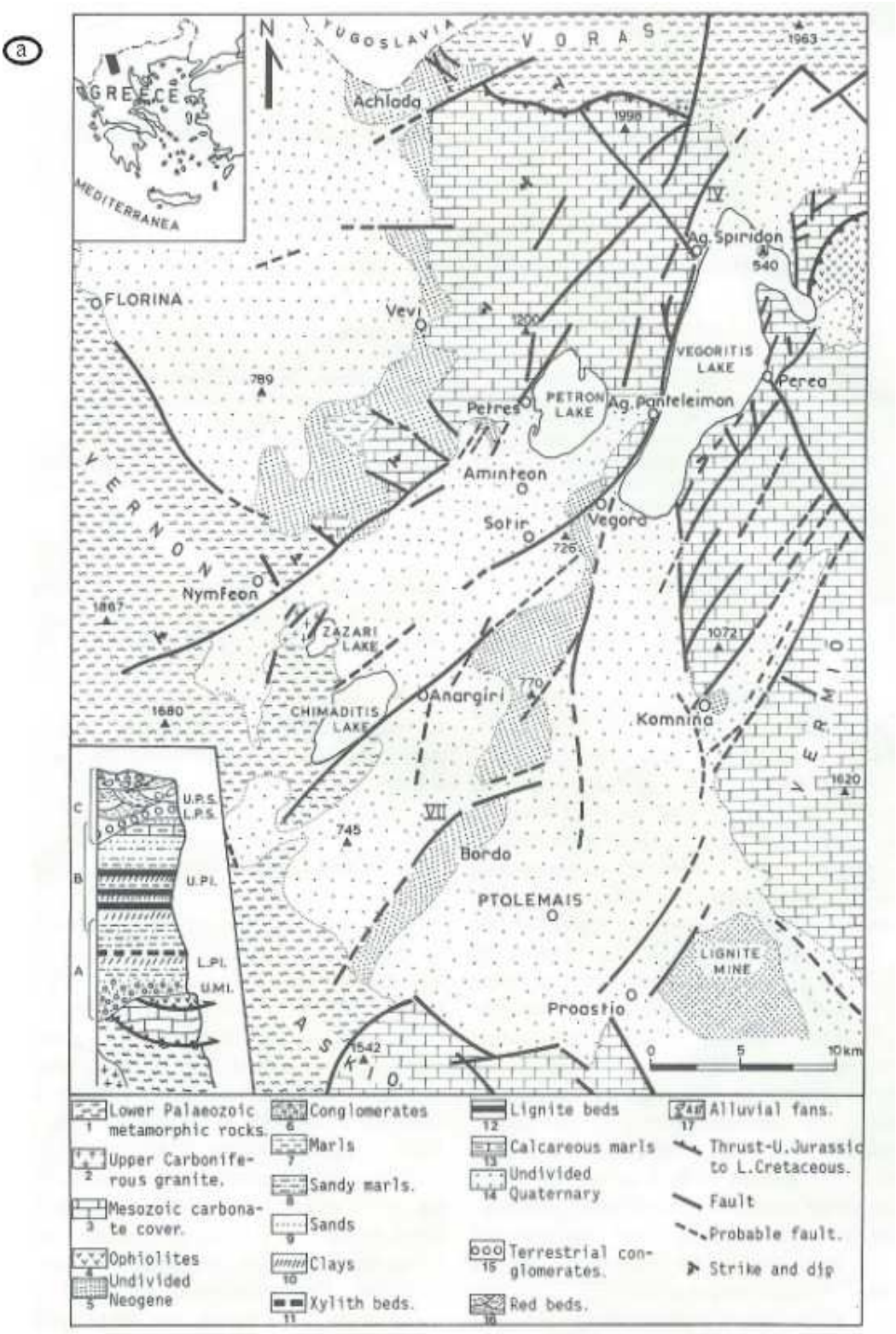

FIG. 1. (a) Tectonic map and stratigraphic section of the Florina–Aetos–Ptolemais basin.

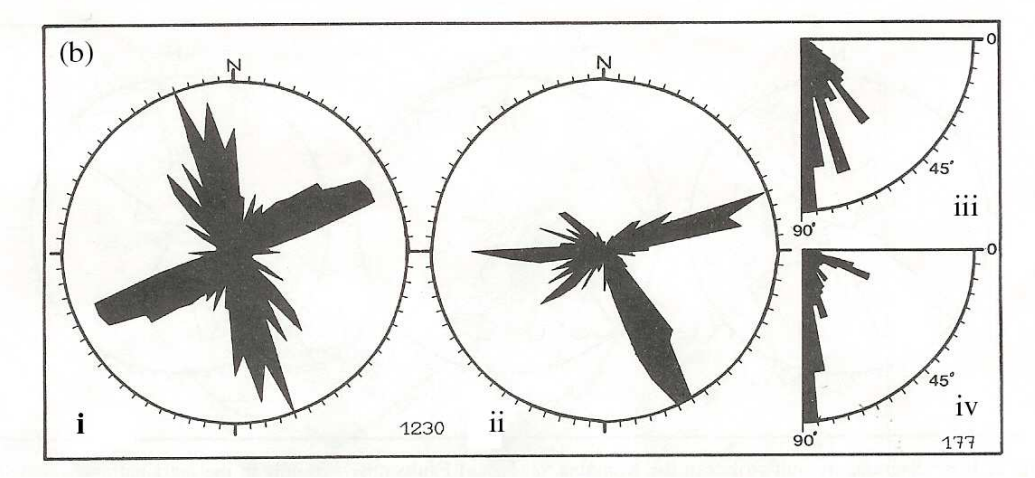

FIG. 1.(b) Rose diagram showing the distribution of faults in Florina–Aetos–Ptolemais basin. (i) Strikes, showing the two main directions NW-SE and ENE-WSW. (ii) Dip direction indicating that the majority of the faults dip SSE and ENE. (iii) Circular histogram where the dip angles of the faults range from 45° to 90° while the majority are high angle dip slip faults (85° – 90° dip). (iv) Pitches of striation of 177 selected representative faults; the majority are dip slip typical normal faults (85° – 90° pitches) meso- and mega-scale and only few meso-scale accommodation structures show oblique slip sense of movements.

are known. These parameters are fixed during the minimisation steps of the fitting error (Rijo, 1977). However, this approach effectively requires that prior geological knowledge should be transformed successfully into compact geoelectrical information and this is not always an easy task.

Sixty-four VES situated on a near regular grid were measured at the area of interest (Figure 2). Initial interpretations were performed using the Zohdy's algorithm (Zohdy, 1989). The IPI2WIN program (Bobatchev et al., 2001), which is based on a non-linear optimisation algorithm using Tikhonov's regularized technique, was used as the main interpretation tool. The interactive nature of the software as well as its ability of simultaneous sounding interpretation proved particularly helpful in to assuring that the interpretations are geologically meaningful.

Final interpretations were produced after finding a representative resistivity for the bedrock and by fixing the resistivity of the half-space during the inversion procedure. Results were combined to form pseudo2-D, 3-D images of the subsurface resistivity. The resulted interpretations are in very good agreement with the existing drill hole information (Koutsinos et al, 1997) and provide useful information about the geological and tectonic setting of the studied area.

GEOLOGICAL SETTING

The pre-Neogene rocks of the Florina–Amynteon–Ptolemais broader basin and surrounding areas are part of the North Pelagonian geotectonic zone, which consists of Palaeozoic crystalline basement, Mesozoic carbonate cover and ophiolites (Mountrakis, 1984). Some of the long faults of the area, which show obvious neotectonic activity in the margins of the Neogene basin, were initially created during Tertiary-folding phases and reactivated in neotectonic times. The basin has tectonic origin and is created along a pre-existed syncline.

The Neogene–Quaternary sediments, which fill up the Amynteon–Ptolemais basin,

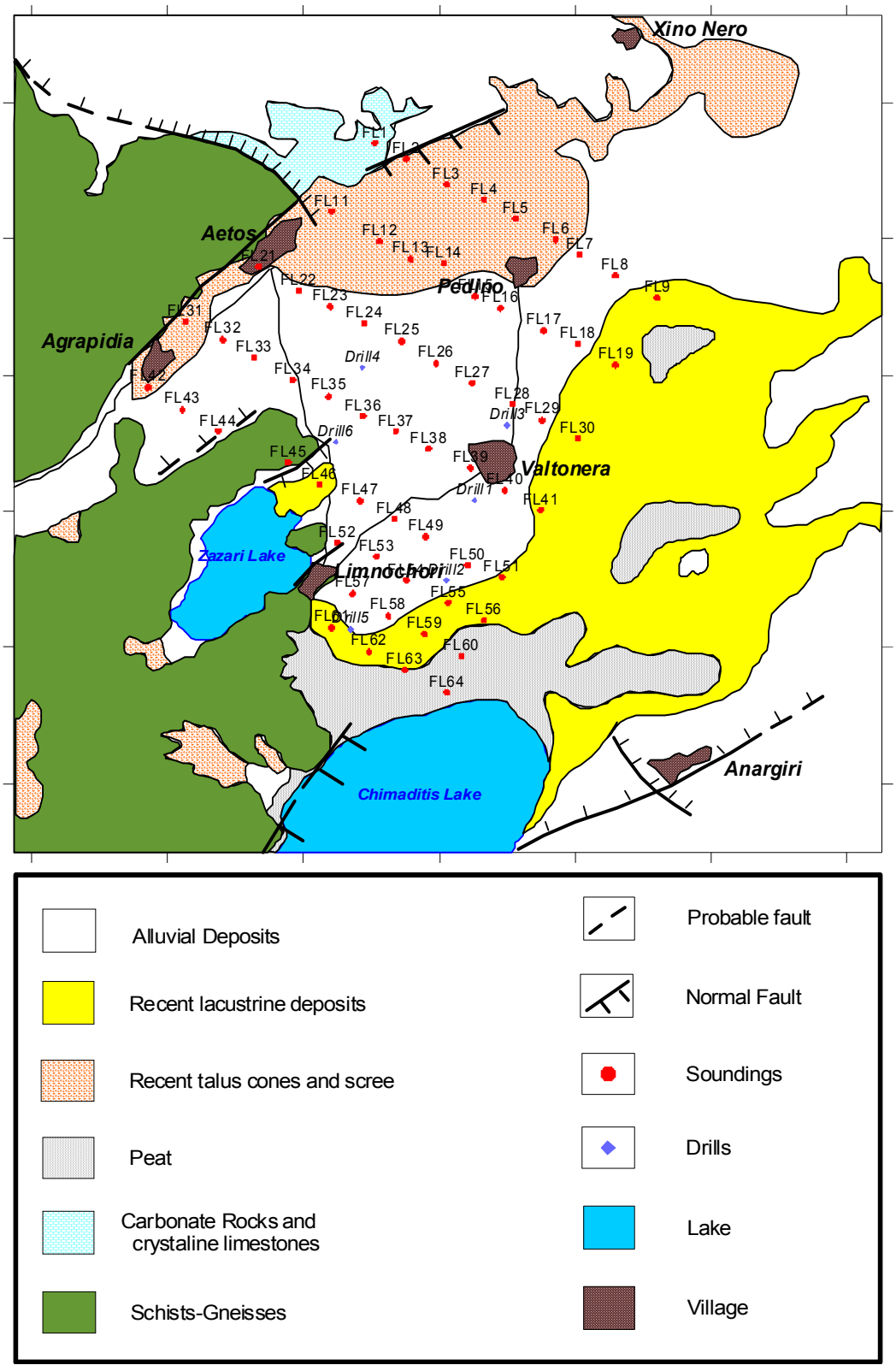

FIG. 2. Simplified map showing the VES centres and the main geological formations in the area of study.

overly uncomfortably both the Palaeozoic metamorphic rocks and the Mesozoic crystalline limestone. They are continental sediments deposited in a lacustrine environment mainly. After detailed stratigraphic work carried out by Anastopoulos and Koukouzas (1972), Koukouzas et al. (1979) and others, these sediments have been divided into the following lithostratigraphic formations (Pavlides and Mountrakis 1987; Koufos and Pavlides 1988 and reference therein):

a. The first (lower) formation consists at its base of conglomerates, containing pebbles of metamorphic rocks, which pass transitionally upwards into a marly layer consisting of marls, sandy marls, clays and some characteristics xylith beds.
b. The second (middle) formation is an argillaceous one containing some thick lignite beds. Alternating with the lignite beds are clays, marls, sandy marls, sands and lacustrine calcareous marls.
c. The third (upper) formation represents the Quaternary deposits, which consist mainly of fluvioterrestrial conglomerates, alluvial fans, scree and recent river deposits.

The dating the onset of the basin formation by means of the oldest sediments could be determined in the stratigraphical data. As mentioned earlier the oldest known sediments of the basin, mainly from borehole samples and, secondly from outcrop observations, are the basal conglomerates. These pass transitionally upwards into marly layers which have been determined as of late Miocene–early Pliocene age. Hence a Middle to late Miocene age for the initial creation of the basin is the most likely (Anastopoulos and Koukouzas 1972; Pavlides and Mountrakis 1987; Koufos and Pavlides 1988).

Numerous faults affect the pre-Neogene rocks and intersect all the above-mentioned Neogene–Quaternary formations. The studied faults could be subdivided into two categories (Pavlides, 1985; Pavlides and Mountrakis 1987). The first includes the faults observed only in the Plio–Quaternary sediments of the basin (NE-SW to ENE-WSW); the second includes the faults observed in the margins of the basin, and continue into the sedimentary layers of the basin (NNW-SSE mainly). Most of these faults are dip-slip typical normal structures and some of them show oblique-slip normal fault character (Fig. 3).

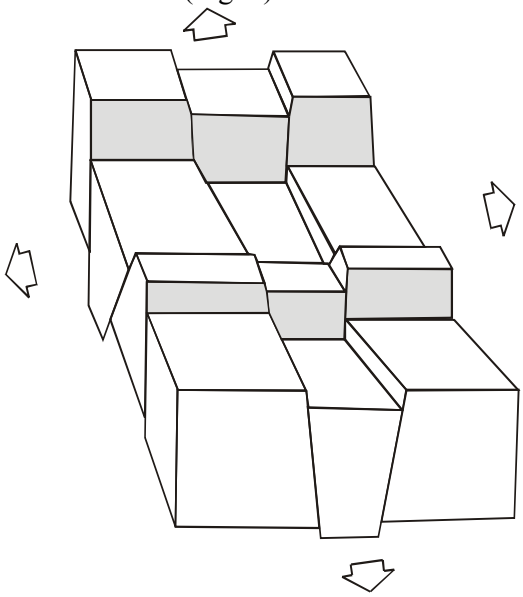

FIG. 3. Typical tectonic model of the studied area with high angle faults shaping dip slopes and "horst-graben" regime, as well as in some cases tilted blocks

As suggested by the geological map of Figure 1, the large marginal NW-SE to NNW-SSE trending is difficult to be located (see the Aetos NW-SE fault) as they are covered by the sediments of the basin and can be detected mainly by boreholes or geophysical investigation. In the contrary the NE-SW trending faults dominate the topography and exhibited typical geomorphological characteristics of recent neotectonic or either active faults. Some faults of the NE-SW direction have been activated recently by weak (Pavlides and Simeakis 1988) and strong earthquakes (Pavlides et al. 1995; Mountrakis et al. 1998). The chronology of faulting has been

established by field evidence for successive fault motions using geometrical and geomorphological criteria and by taking into account stratigraphic data. These were created during the Pliocene. Numerous others with a NE-SW trend cut through the whole Pliocene series and continue into the Lower Pleistocene fluvio-terrestrial conglomerates. In addition, syn-sedimentary fault structures were observed in Pleistocene deposits with the same NE-SW direction (Pavlides, 1985; Pavlides and Mountrakis 1987).

After the completeness of the Alpine orogenic cycle (late Oligocene-early Miocene) the typical continental crust of the region failed into an NE-SW (σ3 trend) extensional regime due mainly to the post-orogenic collapse. It has been shown by quantitative tectonic analysis in the broader region (Pavlides, 1985; Pavlides and Mountrakis 1987; Caputo and Pavlides1993). The result was the re-activation of the NW-SE trending mainly faults and the initial creation of the broader main basin.

A new extensional phase with a NW-SE direction of extension (σ3) took place during early to middle Pleistocene times and caused the most recent block – faulting in the area, which is particularly intensive in the Plio-Pleistocene sediments of the basin. It is very possible that this younger tectonism has continued until present times, as the very recent and unconsolidated sediments, which have been affected by faults, indicate it.

The main faults that dominate the investigated area are the Petron–Xino Nero-Aetos-Nymfeo fault. This long fault divides the broader basin into two sub-basins, the northern Florina and the Amynteon one. The studied area is the southwestern edge of Amynteon basin and lies between Zazari and Chimaditis lakes and Anargiroi, Nymfeon and Aetos villages (Fig. 1). Other faults of NE-SW orientation, arising from the geological map, are the Vegoritis fault, the Chimaditis – Anargiroi fault and some minor structures.

The studied area is occupied by Neogene and Quaternary (lower Pleistocene to Holocene) sediments of various thickness values (few meters up to 400 meters). We can distinguish two distinct horizons that differ in age and composition and they have normal transition to each other. An intense period of tectonic movements was followed after the deposition of the Pliocene sediments. This tectonism, which contributed to the huge rupture of the area, in correlation with the erosion, had as result the creation of rift tectonics ("horsts" and "grabens") of the sub-stratum and the creation of the Chimaditis – Zazari basin. Peats, peaty clay and recent lacustrine deposits dominate in the vicinity of Zazari and Chimaditis lakes. These deposits thought that they constitute the impermeable cover to the regional geothermal potential that is trapped between the bedrock and the basement conglomerate.

Water drill holes, made over the tertiary sediments, testify the existence of large renewable and exploitable aquifers (reservoirs) with large porosity at low depths (Koutsinos et al, 1997).

At the center of the Amynteon basin, both basin and aquifers becomes deeper with higher porosity. Near the basin's margins, the aquifers are found in the shallow depths and consequently have lower porosity.

MEASUREMENTS AND DATA PROCESSING

A total number of 64 Schlumberger soundings were measured in the studied area (Fig. 2) having a maximum AB/2 separation of 1000 m. The sounding centers are 500 m apart and were situated in 8 parallel sections in a 3x4 km NW-SE grid while the intra-section distance was 500 and 1000 m. Combined interpretations were carried out by considering almost collinear sounding centers both with NW-SE (Figure 4a) and SW-NE (Figure 4b) orientations.

Data quality was particularly good as suggested by the low standard deviations (0.5-1%) recorded in the field. The relatively smooth behavior of all recorded sounding curves indicate that the geology of the area fits the assumptions of 1-D interpretation. This was also verified later by the low RMS

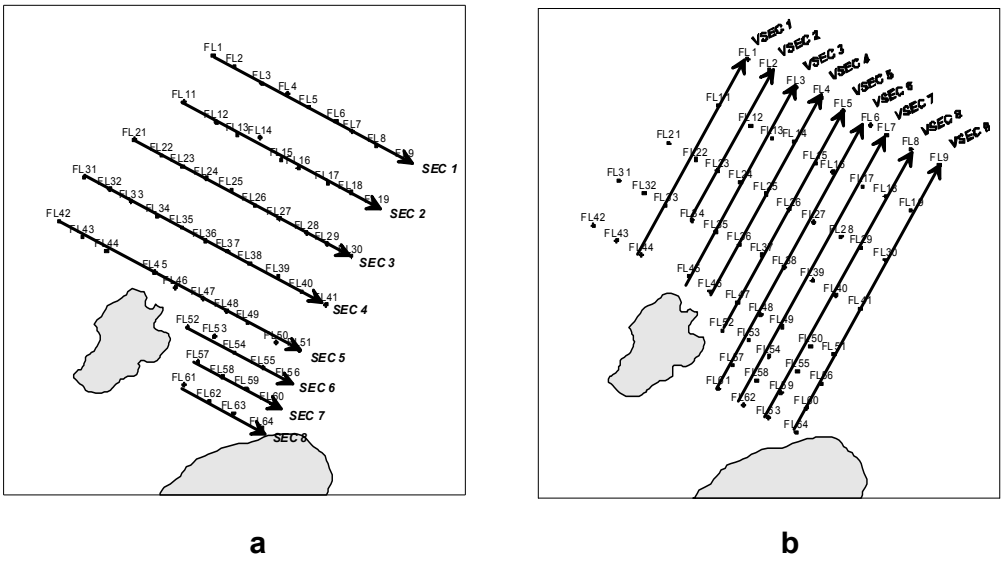

FIG. 4. The interpreted geoelectrical sounding sections (a) sections with NW-SE orientation (b) sections with SW-NE orientation.

errors (<1%) obtained by all sounding interpretations.

The initial processing of the sounding data involved interpretation using the Zohdy algorithm (Zohdy, 1989). Despite its theoretical simplicity this algorithm is known to produce smooth models representative of the subsurface resistivity distribution. The individual sounding results were combined to produce pseudo-2D sections of the subsurface resistivity. Such a section (SEC4 of Figure 4a) is presented in Figure 5.

We used the IPI2WIN program (Bobatchev et al., 2001) for the main interpretation of the VES data. The software allows the user to present multiple sounding interpretations in a single window and thus interpretations of adjacent VES can be represented as a single geological structure rather than a set of independent objects. Further, it enables interactive interpretation enabling the user to choose, from a set of possible models, the one that both fits the VES data and produces sectional interpretations that are geologically reasonable.

Initially we tried to fix the depth of the last layer, since there was relatively accurate geological information from the area (6 test drills) in order to coincide with the geological background (schist gneiss). Then, we invert data to retrieve the bedrock's resistivity. Yet, the presence of a conglomerate formation, of varying composition and compaction, just above the bedrock suggest that this formation could locally behave geoelectrically similar to the bedrock. As a result, it was not possible to define the bedrock limit exactly and eventually we retrieved inversion results that produced quite varying resistivity values for the bedrock.

Instead of using the drill information to constrain the inversion directly we used the following approach to overcome the problem. A large number of VES, which appeared to be affected by the bedrock, was selected. The selection criteria involved the shape of the sounding curve, the drill information and the existing interpreted resistivity sections obtained using the Zohdy technique. Initially, we performed individual unconstrained inversions, just to the selected VES, by providing a simple initial model extracted from the results of the Zohdy's technique. Inversion results produced quite consistent resistivities for the bedrock that ranged between 1000 and 2000 ohm-m.

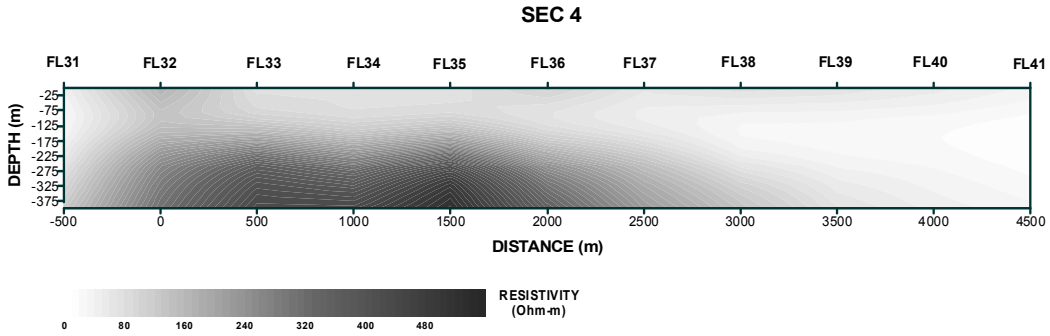

FIG. 5. Initial interpretation of the geoelectrical sounding section 4 (SEC4 of Figure 4a) using Zohdy's algorithm.

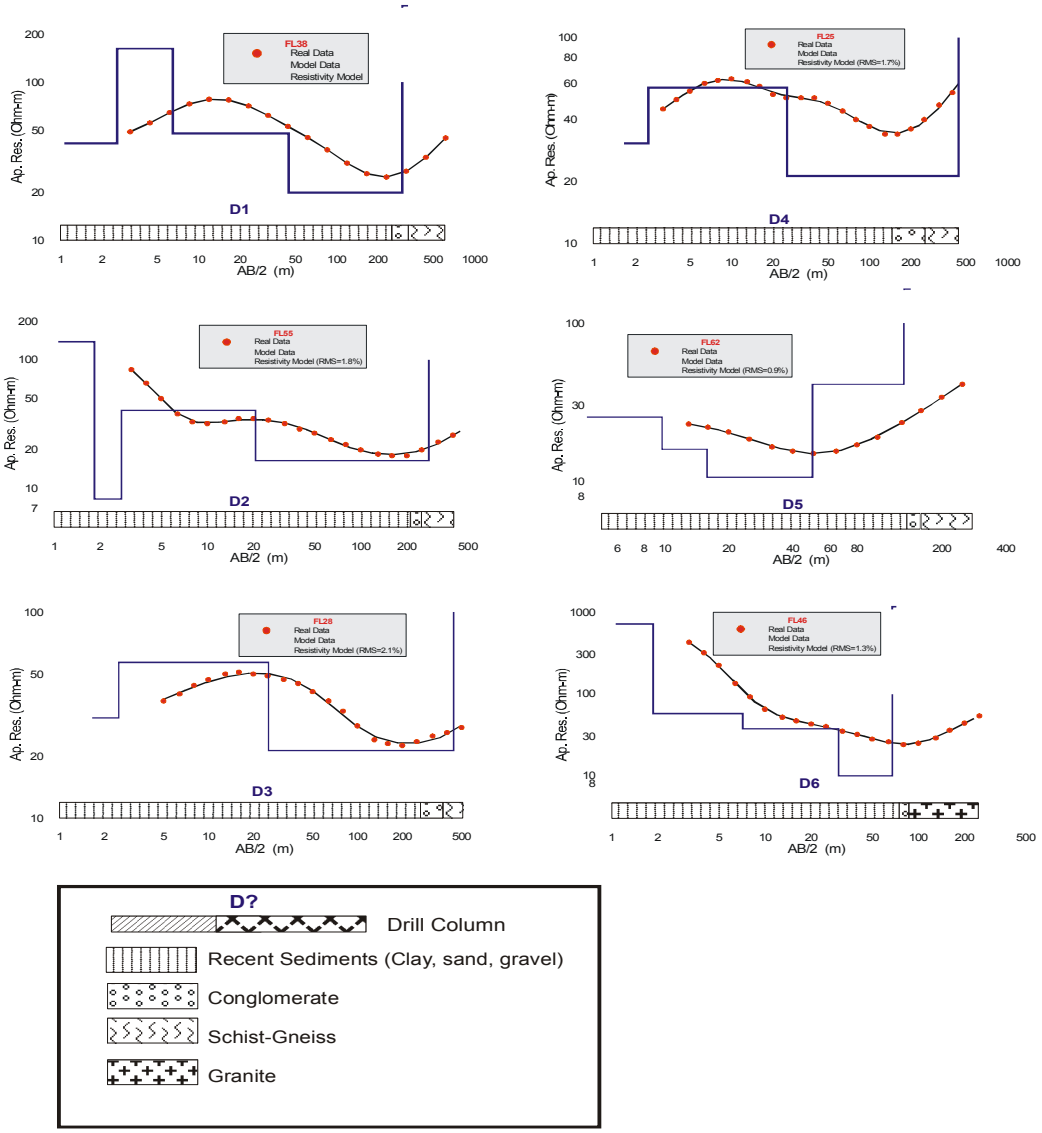

FIG. 6. Correlation of selected VES interpretation with the nearest test-drills columns (X-axis).

We then performed individual inversions for all collected VES by fixing indiscriminately the resistivity of the half-space to be 1500 ohm-m. It is worth mentioning that this approach did not create problems in areas for which no high resistivity half space is justified by data and geology. In these cases inversion produced a depth for the resistive half-space, which is well below the VES depth of investigation (>400 m) and thus it can be safely ignored.

Since geoelectrical interpretations were not constrained *a priori* to fit the drill information, all six existing drills columns are presented against the produced interpretations and fits of the VES that are the nearest to the test drills positions in order to test the validity of the interpretation approach (Figure 6). The VES interpretations are in very good agreement with the drillings as far as the location of the bedrock is concerned and this suggests that the final interpreted results can be considered reliable.

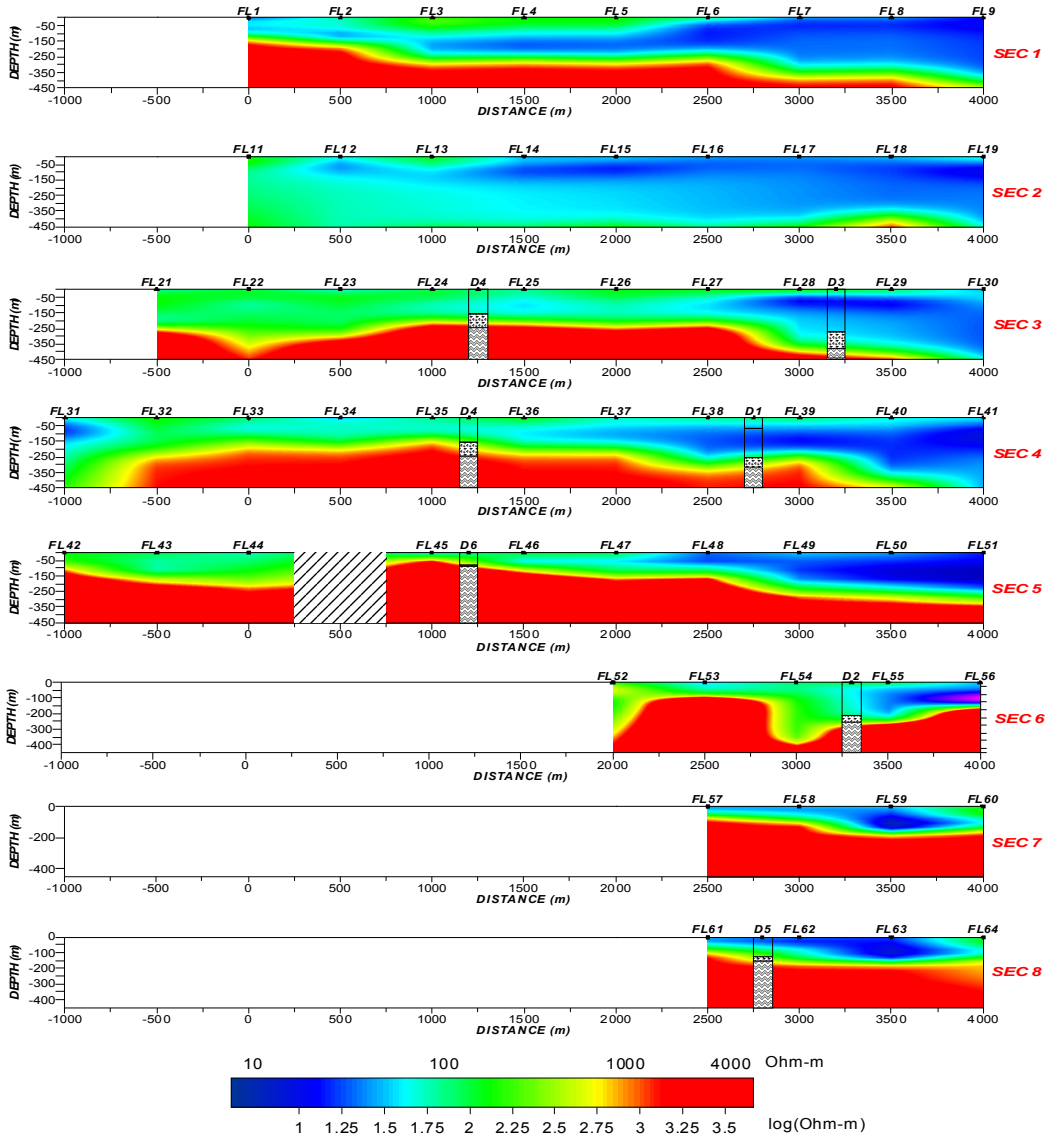

FIG. 7. Pseudo-2D subsurface resistivity sections of the NW-SE sections SEC1-SEC8 (see also Figure 4a).

INTERPRETATION AND DISCUSSION

Based on the produced sounding interpretations the following correlation between the geological and geoelectrical formations can be considered: The topsoil layer (0-3 m) has a varying resistivity due to its highly variable composition.

The main sedimentary formation (Pleistocene to Holocene) consists of clays and alternations of relatively thin layers of sands and gravels, which effectively cannot be identified as individual geoelectrical layers.

The geoelectrical formation, which corresponds to the sedimentary series, has a resistivity ranging from 15 to 60 ohm-m and can be distinguished into two sub-formations of higher and lower resistivity ranging from 30-60 ohm-m (top formation) and 15-30 ohm-m (bottom formation) respectively. This resistivity reduction could be attributed mainly to a lithological variation since the formation is becoming more argillaceous with depth, and partly due to the increase of the geothermal gradient (Koutsinos et al, 1997). The latter is suggested by geothermal exploration in the area, which indicates an average increase of 15^{o}C in temperature at a depth of 300 m. This differentiation between the above mentioned sedimentary series is partly arbitrary. It concerns geoelectrical layers with overlapping range of resistivity values.

The bedrock formation is clearly identified as a geoelectrical layer and was fixed to be of resistivity 1500 ohm-m. No distinction of the bedrock lithology (schist-gneiss or granite) can be made due to the similar range of resistivities that these formations present.

The drill information suggests the existence of a conglomerate formation of varying composition, thickness and compaction, which is intermediate between the sediments and the bedrock (Koutsinos et al, 1997). This formation cannot be recognized within the interpreted VES results as an individual geoelectrical unit. Whenever we tried to incorporate this layer into the initial inversion model it vanished in the inversion results. A possible explanation is that in areas of low compaction this formation has resistivities similar to the overlaying sediments but in cases of higher compaction it behaves electrically similarly to the bedrock.

The interpretation results were combined to form pseudo-2D subsurface resistivity sections of the studied area. Figures 7,8 depict NW-SE sections (SEC1-SEC8, Fig. 4a) and SW-NE sections (VSEC1-VSEC9, Figure 4b) respectively.

In Figure 9 the interpretation results were combined to produce pseudo-3D depth slices for depths ranging from 50 m to 450 m.

Finally, in Figure 10 a 3-D image of the surveyed area depicting the relative depths of the geological background is shown. Note, that the results of Figure 10 are in very good agreement with the typical tectonic model of the studied area (Figure 3) and fully verify the tectonic structure proposed by Pavlides (1985) and Pavlides and Moundrakis (1987).

As it can be seen from the results of the geophysical interpretation two main faulting systems can be identified. The first has a NW-SE direction and it appears to be between the Aetos-Valtonera axis and the Pedino village. This appears to be associated with the known tectonic contact (Pavlides, 1985) between the schists and marbles to the North of the Aetos village. This faulting system appears to be responsible for the lowering of the bedrock at the eastern part of the studied area.

The second faulting system has almost a N-S direction (Pedino-Valtonera axis) and it sets the western limit of the bedrock prior to its dipping.

At the southern part of the studied region it is worthwhile mentioning the existence of a localized dipping of the bedrock, which appears to be associated to the formation of the Zazari Lake.

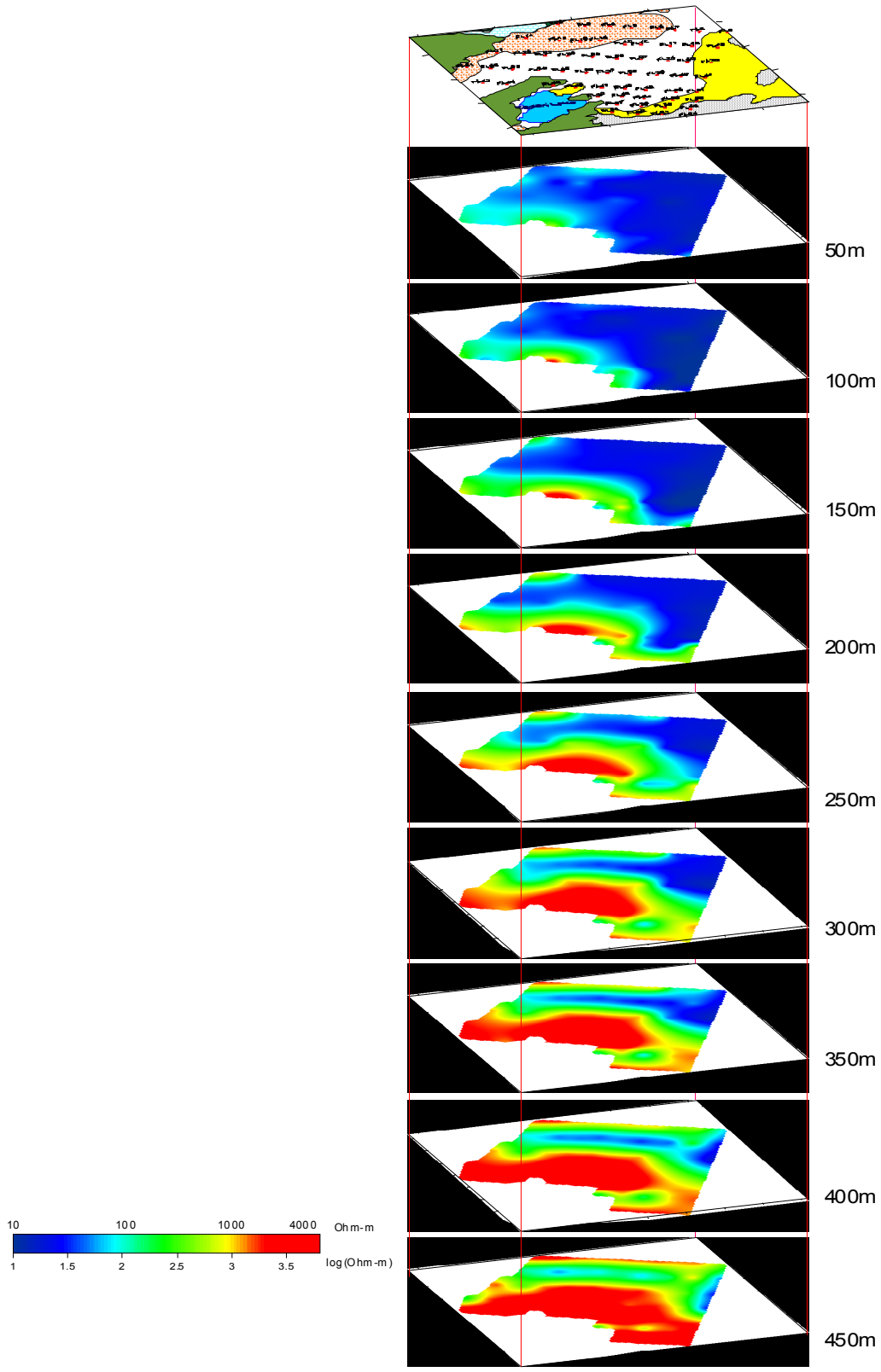

FIG. 9. Interpreted resistivity results presented in a 3D layout as depth slices from a relative depth of 50 m to 450 m.

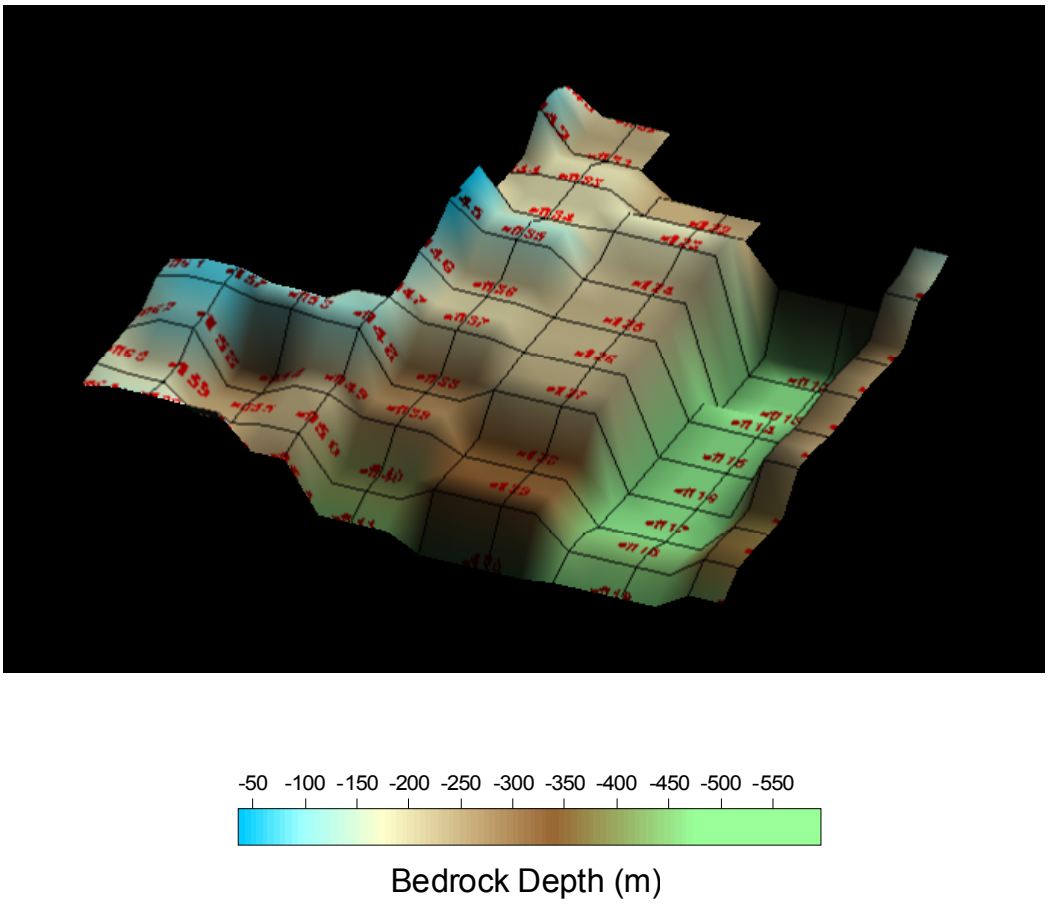

FIG. 10. 3-D image of the surveyed area depicting the relative depths of the geological background.

CONCLUSIONS

Interactive interpreting of VES and careful consideration of the existing geological information leads to increasingly reliable VES interpretations. Further, by combining the 1-D interpretation results and presenting them into pseudo-2D and 3D subsurface resistivity image certainly helps into forming a clearer picture about the studied area.

We suggest that for large-scale surveys, which target to intermediate depths of investigation (100-300 m), VES measurements remain a practical and effective subsurface imaging tool. Compared to the increasingly popular 2-D resistivity surveys VES at low-resolution scale and intermediate investigation depths is certainly less costly and almost equally effective.

Geophysical results can't be accepted alone for a final interpretation of the Amynteon-Zazari-Chimaditis sub-basin, but in association with geological, geomorphological and borehole data, in order to establish the type and the dimension of faulted area and basin's floor. The structure of the sub-basin, which is the structure of the greater basin in smaller scale, from surface geological data, boreholes and mainly from the geoelectric ones are characterized by rift tectonics and normal faults activated into two distinct tectonic phases. They are high angle faults shaping dip slopes and "horst-graben" regime, as well as in some cases tilted blocks. The resulted geophysical image is in very good agreement with the existing geological and tectonic information for the area and indicates the ability of geophysical surveying to aid and verify the geological

interpretations. Further the results allowed us to verify the continuation of known faults and to obtain new structural information about the studied area. The results indicate that despite the increased use of 2D electrical surveys, 1-D VES measurements are still a very useful tool for larger scale applications.

REFERENCES

Anastopoulos, J., and Koukouzas, C., 1972, Economic geology of the southern part of Ptolemais lignite basin (Macedonia, Greece): Geol. And Geoph. Research, IGME, Athens, No 16, p. 1-189, (in Greek).

Basokur, A.T., 1990, Microcomputer program for the direct interpretation of resistivity sounding data: Computers & Geosciences,**16**, 587-601.

Basokur, A T., 1999, Automated 1D interpretation of resistivity soundings by simultaneous use of the direct and iterative methods: Geophysical Prospecting, **47**, 149-177.

Bobatchev, A., 1992, Electrical sounding of geological media: Moscow University Edition, part 2, 200 pp. (in Russian).

Bobatchev, A, Modin, I. and Shevnin, V., 2001, IPI2WIN v.2.0, User's manual.

Caputo, R. and Pavlides, S., 1993, Late Cenozoic geodynamic evolution of Thessaly and surroundings (central – northern Greece): Tectonophysics, **223**, 339-362.

Ghosh, D. P., 1971, The application of linear filter theory to the direct interpretation of geoelectrical resistivity sounding measurements: Geophysical Prospecting, **19**, 192-217.

Inman, J. R., 1975, Resistivity inversion with ridge regression: Geophysics, **40**, 798-817.

Koefoed, O., 1979, Geosounding principles, 1, Resistivity Sounding Measurements: Elsevier, Amsterdam.

Koufos, G. and Pavlides, S., 1988, Correlation between the continental deposits of the lower Axios valley and Ptolemais basin: Bull. Geol. Soc. Greece, **22**, 9-19.

Koukouzas, C., Kotis, T., Ploumidis, M. and Metaxas, A., 1979, Coal exploration of Anargiri area, Aminteon (W. Macedonia), Mineral Deposit Research. IGME, Athens, No 9, p. 1-69, (in Greek).

Koutsinos, S., Kolios, N., Karidakis, G. and Atzemoglou, A., 1997, Preliminary results of geothermal research in lake Zazari and Chimatidis region, Florina prefecture, Macedonia, Greece. IGME Report (in Greek).

Kunetz, G., 1966, Principles of direct current resistivity prospecting: Gebruder Borntaeger, Berlin.

Mountrakis, D., 1984, Structural evolution of the Pelagonian zone in North - Western Macedonia. The Geological Evolution of the Eastern Mediterranean, Special Publication of the Geological Society, No 17, p. 581-590.

Mountrakis, D., Pavlides, S. Zouros, N., Astaras, TH. and Chatzipetros, A., 1998, Seismic fault geometry and kinematics of the 13 May 1995 western Macedonia (Greece) earthquake: J. Geodyn. Spec. Issue Pavlides & King (Eds), 26, 2-4, 175-196.

Pavlides, S., 1985, Neotectonic evolution of the Florina - Vegoritis – Ptolemais basin (W. Macedonia, Greece), PhD thesis, Aristotle University of Thessaloniki, 265 pp. (in Greek with Engl. abs).

Pavlides, S. and Simeakis, K., 1988, Neotectonics and active tectonics in low seismicity areas of Greece: Vegoritis (NW Macedonia) and Melos isl. Complex – Comparison, Ann. Geol. des Pays Hellen., 33, pp. 191-176.

Pavlides, S. and Mountrakis D, 1987, Extensional tectonics of North-

western Macedonia, Greece, since the late Miocene. Journal of Structural Geology, **9**, 385-392.

Pavlides, S., Zouros, N., Chatzipetros, A. Kostopoulos, D. and Mountrakis, D., 1995, The 13 May 1995 western Macedonia, Greece (Kozani-Grevene) earthquake; preliminary results: Terra Nova, **7**, 544-549.

Rijo, L., 1977, Modelling of Electric and Electromagnetic data: Ph.D. Thesis. University of Utah.

Zohdy, A. A. R., 1989, A new method for the interpretation of Schlumberger and Wenner sounding curves: Geophysics, **54**, 245-253.